

Phenol removal from aqueous solution by carbon xerogel

Liana Alvares Rodrigues · Tiago Moreira Bastos Campos ·
Manoel Orlando Alvarez-Mendes · Aparecido dos reis Coutinho ·
Kumiko Koibuchi Sakane · Gilmar Patrocínio Thim

Received: 27 November 2011 / Accepted: 8 March 2012 / Published online: 20 March 2012
© Springer Science+Business Media, LLC 2012

Abstract Carbon xerogel (CX) was used for phenol adsorption from aqueous solution. CX was synthesized by sol–gel polycondensation of resorcinol with formaldehyde using sodium carbonate (Na_2CO_3) as catalyst. Then, it was dried by convective drying technique and pyrolyzed under inert atmosphere. Phenol adsorption kinetics was very fast, what was attributed to the presence of open pore structure. The kinetic studies showed that the adsorption process could be fitted to a pseudo-second-order model and the particle diffusion process is the rate-limiting step of the adsorption. The phenol removal was maximum and unaffected by pH changes when the initial pH of the phenol solution was in the range of 3–8. The optimum adsorbent dose obtained for phenol adsorption onto CX was $0.075 \text{ g}/50 \text{ cm}^3$ solution. The Langmuir model described the adsorption process better than the Freundlich isotherm model and the monolayer adsorption capacity is 32 mg g^{-1} . Among the desorbing solutions used in this study, the most efficient desorbent was EtOH (100 %) which released about 87 % of phenol bound with the CX.

Keywords Carbon xerogel · Phenol · Adsorption

1 Introduction

Phenolic compounds are common contaminants in wastewater, being generated from petroleum and petrochemical, coal conversion, pulp and paper, plastic, rubber-proofing, disinfectant, pharmaceutical, steel and phenol producing industries [1–4].

Phenol compounds are considered priority pollutants since they are harmful to organisms in low concentrations and many of them are classified as hazardous pollutants because of their potential to harm human health [5–7]. The ingestion of phenol contaminated water causes protein degeneration, tissue erosion, paralysis of the central nervous system and also damages in the kidney, liver and pancreas of the human bodies [8]. Their presence in water supplies is noticed by its bad taste and odor [9, 10]. Therefore, removal of phenols from water and wastewater is an important issue in order to protect the public health and the environment.

Phenol contaminated water can be treated by several physicochemical and biological techniques, such as: solvent extraction, ion exchange by resins, chemical oxidation by ozone, aerobic or anaerobic biodegradation, etc. However, the phenol adsorption on activated carbon process is the most used nowadays, since it is the most effective technique for phenol removal [11–14]. The activated carbon adsorption properties are attributed to its physical and chemical structure [15].

Recently, carbon gel has been used as carbon adsorbent [16–18]. Carbon gels are constituted of meso and/or microporous, distributed in a network structure, because of these characteristics, carbon aerogels show unique properties,

L. A. Rodrigues (✉) · T. M. B. Campos · G. P. Thim
Instituto Tecnológico de Aeronáutica-ITA/CTA, Praça Mal.
Eduardo Gomes 50, São José dos Campos, São Paulo CEP
12228-900, Brazil
e-mail: lika_eng@yahoo.com.br

M. O. Alvarez-Mendes · A. Coutinho
Laboratório de materiais carbonosos, Universidade Metodista de
Piracicaba, Rod. SP 306, Km 01, Santa Bárbara d'Oeste,
São Paulo 13450-971, Brazil

K. K. Sakane
Universidade do Vale do Paraíba, Avenida Shishima Hifumi
2911 Urbanova, São José dos Campos, SP CEP 12244-000,
Brazil

such as: low mass density, continuous porosity, high surface area and high electrical conductivity. They can be produced in monolithic, powder and sheet form, providing excellent wastewater purification treatment and cost effective manner [17].

For any sorbent to be feasible, it must combine high and fast adsorption capacity with inexpensive regeneration. The present work describes the syntheses of carbon xerogel (CX) based on resorcinol/formaldehyde (RF) method. The obtained material was applied to the study of kinetics and isotherm aspects of phenol adsorption from aqueous solutions onto CX.

2 Methods

2.1 Preparation of carbon xerogel (CX)

Carbon gel was produced from the polycondensation of resorcinol and formaldehyde in water with sodium carbonate as catalyst. A solution of resorcinol and formaldehyde containing 5 % (w/v) of sodium carbonate was prepared, in which the resorcinol/formaldehyde molar ratio was set to $R/F = 0.5$, and the resorcinol/catalyst molar ratio was set to $R/C = 25$. The solution was sealed in a flask, mechanically stirred for 30 min and then put into an oven for 3 days at 80 °C. After the drying step, the hydrogel was cooled at room temperature. The hydrogel was immersed in acetone for a day, the solvent was filtered and fresh acetone was added to the remaining gels; this procedure was repeated three times. The gels were maintained at 150 °C until a constant weight was achieved. This dry gel is called as RF xerogel. Finally, the carbon xerogel (CX) was formed by the RF xerogel pyrolysis at 750 °C for 1 h in an Argon atmosphere with heating rate of 10 °C min⁻¹.

2.2 Characterization

A Raman microscope (Renishaw 2000 with $\lambda = 514.5$ nm) was used to record the Raman spectra of the CX particles. This technique allowed recording the Raman spectra of the individual particles to characterize the types of chemical bonds that constitute the material.

FTIR spectrum was collected on a FTIR spectrometer (Perkin Elmer Spectrum GX). The IR spectrum was the average of 12 scans at a speed of 2 s per scan in the range of 400–4,000 cm⁻¹. The resolution of the spectrometer was set to 4 cm⁻¹. Infrared absorption spectrum of the dried xerogel was obtained within KBr matrices. Prior to the FTIR analysis ≈ 50 mg of crushed dried gel was added to ≈ 150 mg KBr. The resulting sample was mixed vigorously, and then the sample was pelletized into a 1 cm diameter disc under a pressure of 10 tons.

Nitrogen adsorption isotherm at 77 K was determined in an Autosorb-1MP gas analyzer (Quantachrome Instruments). Using the Brunauer, Emmett, and Teller (BET) equation, data from the isotherm was used to determine the BET surface area. The micropore area was obtained by applying the t -plot method. The total pore volume was determined by converting the volume adsorbed at the saturation point $P/P_0 \sim 0.99$ into liquid volume, whilst the micropore volume was calculated at the point of interception of the linear region of the t -plot after saturation of the micropores. The mesopore volume was calculated from the difference between the total pore volume and the micropore volume. The pore size distribution of AAC was determined based on the non-local density theory (DFT).

The sample used for SEM observation was prepared by dispersing some products in ethanol followed by ultrasonic vibration, then placing a drop of this dispersion on a copper grid.

The point of zero charge (pH_{pzc}) was determined using a batch equilibration method, previously described in Ref. [19]. Initial pH values (pH_i) of 25 cm³ of KNO₃ solutions (concentrations 10⁻¹ and 10⁻² M) were adjusted in pH range of 2–8 using 0.1 M of HCl or NaOH. Then, 0.05 g of CX was added to each sample. Equilibration was carried out in a thermostatic orbital shaker for 24 h at 298 K. The dispersions were filtered and the final pH of the solutions (pH_f) was determined. The point of zero charge was found from a plot of ($\text{pH}_i - \text{pH}_f$) versus pH_i .

The contents of the oxygenated chemical groups present on the carbon aerogel surface were determined according to Boehm method [20]. One gram of CX was placed in 25 cm³ of the following aqueous solutions: sodium hydroxide, sodium carbonate, sodium bicarbonate and hydrochloric acid. The vials were sealed, shaken for 24 h and then filtered. The filtrate was titrated with HCl or NaOH for determining the base or acid excess, respectively.

2.3 Adsorption studies

All adsorption studies were carried out by adding 0.075 g of CX sample in a 50 cm³ of phenol aqueous solution under stirring in a thermostatic orbital shaker. The supernatant solution was separated from the adsorbent by filtration. The phenol concentration in the supernatant was spectrophotometrically determined using UV–VIS absorbance spectrophotometry at 269 nm.

The influence of adsorbent contents in adsorption processes was investigated by adding various amounts of CX in several vials of 50 cm³ containing phenol aqueous solution (500 mg dm⁻³) at 298 K for 24 h. For the kinetic studies, 0.075 g of adsorbent were added in 50 cm³ of phenol aqueous solutions (500 mg dm⁻³), the final suspension was

agitated at 298 K for several intervals of time. After each time interval, the phenol concentration was determined using UV–VIS absorbance spectrophotometry at 269 nm.

The effect of pH in adsorption process was studied by the adjustment of the initial pH of phenol aqueous solutions ($C_0 = 500 \text{ mg dm}^{-3}$) to different pH values with 0.1 mol dm^{-3} NaOH or HCl. Adsorption studies were performed with these phenol solutions using the methodology described in the first paragraph.

The isotherm study was carried out in an aliquot of 50 cm^3 of several phenol aqueous solutions, in which the concentrations ranged from 100 to 500 mg dm^{-3} . A pre-determined adsorbent dose was added to each phenol aqueous solution.

2.4 Desorption

The adsorbent used for the adsorption of 500 mg dm^{-3} of phenol solution was separated from the solution by filtration and was gently washed with deionized water to remove phenol molecules that were not adsorbed on CX. Then this adsorbent was mixed with 50 cm^3 of different desorbing agents in different concentrations and agitated in time intervals no longer than the equilibrium time. Different desorbing agents such as; deionized water, NaOH (0.1 M), NaOH (0.25 M), NaOH (0.5 M), EtOH (25 %), EtOH (50 %), EtOH (75 %), EtOH (100 %), were used in order to determine the most appropriate eluant or desorbing solution. The content of the desorbed phenol was determined by the methodology previously described.

3 Results and discussion

3.1 Characterization

A typical Raman spectrum of the pyrolyzed particles (Fig. 1) shows two broad peaks centered at about 1,340 and $1,590 \text{ cm}^{-1}$, which are associated with the vibrations of sp^2 carbon atoms with dangling bonds (defects in the graphitic lattice) [21].

Figure 2 shows the Fourier transform infrared spectroscopy (FT-IR) analysis of the carbon xerogel sample. The broad band centered around $3,600 \text{ cm}^{-1}$ and between 2,500 and 3,000 was characteristic of O–H stretching vibrations involving hydrogen bonding interactions between carboxyl, hydroxylactone, or phenol groups and adsorbed water [22, 23]. The absorption band at $2,900 \text{ cm}^{-1}$ was associated with $\nu_{\text{as}}(\text{C-H})$ and $\nu_{\text{s}}(\text{C-H})$ of methyl and methylene groups [24]. The bands near 1,490–1,500 and 920–950 were assigned with tri-substituted benzene ring [25]. In addition, the band at $1,700 \text{ cm}^{-1}$ may be associated with the C=O stretching vibration from an unreacted aldehyde group

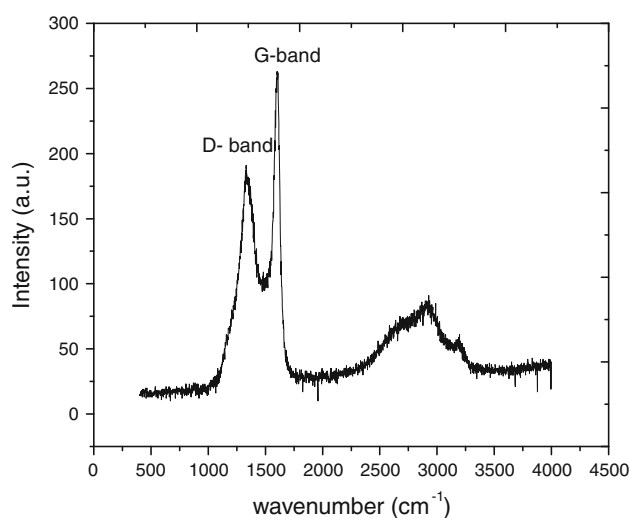


Fig. 1 Raman spectrum of CX

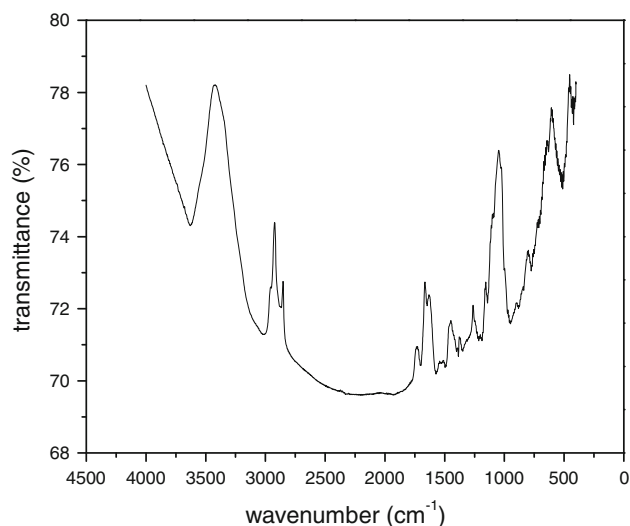


Fig. 2 FTIR spectrum of CX

and/or with the carbonyl generated when formaldehyde underwent a ring-opening reaction [22]. A peak at $1,590 \text{ cm}^{-1}$ was related with carbonyl, ester and quinone groups (C=O) [26]. Besides these functional groups, peaks below 800 cm^{-1} can be assigned to out of plane bending of –OH group and out of plane deformation vibration of C–H moieties of aromatic structures present in CX [27]. C–O–C groups, associated with vibrations of methylene ether bridges between resorcinol molecules, should be found between 1,000 and $1,300 \text{ cm}^{-1}$, and several peaks appear in this interval [28].

Figure 3 shows the nitrogen adsorption isotherm measured at 77 K of CX sample. The isotherm curves shown in Fig. 3 are characteristics of materials constituted by micro

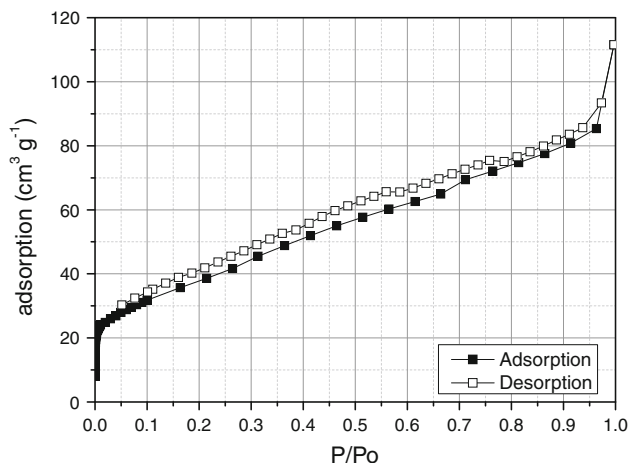


Fig. 3 N₂ Adsorption isotherm of CX

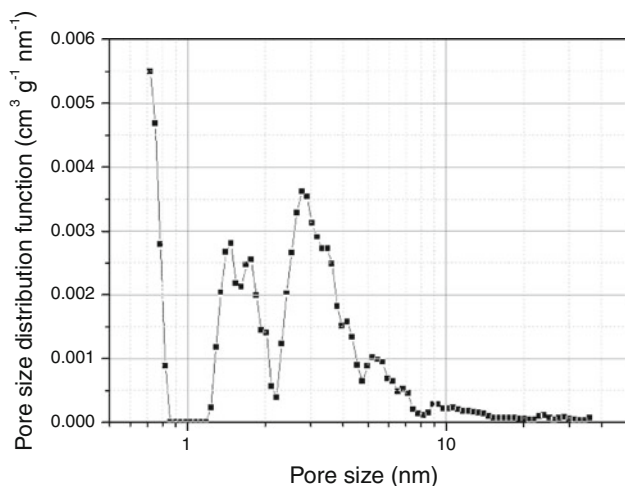


Fig. 4 Pore size distribution of CX

and mesopores and can be classified as types IV, according to IUPAC classification [29]. CX shows the H3 type hysteresis loop which is commonly found for adsorbents constituted of slit-shaped pores or plate-like particles [30]. The BET and micropore surface areas of sample CX is 128 and 110 m² g⁻¹, respectively, i.e., micropore surface area corresponds to 86 % of the BET surface area. Sample CX showed micropore volume equal to 0.100 cm³ g⁻¹ and total pore volume as high as 0.173 cm³ g⁻¹, i.e., 58 % of the total pore volume is associated to micropores.

Figure 4 shows the pore size distribution of sample CX. One can observe a trimodal distribution, where the main peak is located below 1 nm and two other peaks is centered approximately at 1.5 and 3 nm. It can be noticed that due to the sample heterogeneity the average pore diameter is 5.4 nm. However, this material is mostly formed by micropores with pore size around 0.72 nm, indicating that its micropores are in the supermicropore range [31].

Figure 5a, b shows SEM images of the morphology of RF and carbon xerogels, respectively. These figures show that carbonization process have strong influence on the morphology of the material. Sample shows macroporous structures before the carbonization step (Fig. 5a), but it shows needlelike structures with macro-aggregation after carbonization step (Fig. 5b).

The pH value at which the surface charge is zero is called point of zero charge (pH_{PZC}). For amphoteric carbons the surface is positively charged at pH < pH_{PZC} and negatively charged at pH > pH_{PZC} [8]. The pH_{PZC} value determined for the CX obtained in this study was 8.3.

The number of basic sites on the CX surface was calculated from the amount of hydrochloric acid that reacted with CX. The number of acid sites was determined under the following assumptions: that there are only carboxylic, lactonic and phenolic groups on CX; that NaOH neutralizes carboxylic, lactonic and phenolic groups; that Na₂CO₃ neutralizes carboxylic and lactonic groups; and that NaHCO₃ neutralizes only carboxylic groups. The amounts of total acid sites, total basic sites, carboxylic groups,

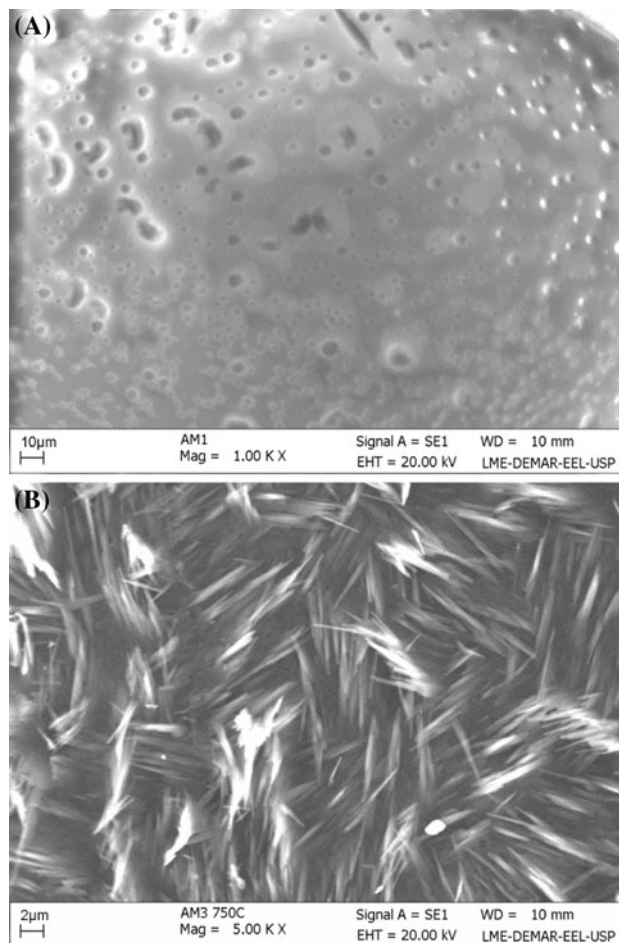


Fig. 5 SEM micrograph of: a RF xerogel; b carbon xerogel

lactonic groups and phenolic groups on CX surface are 0.61, 0.69, 0, 0 and 0.61, respectively.

3.2 Effect of adsorbent dosage

Figure 6 shows the adsorption percentage (%) and adsorption capacity (q_e) of phenol as a function of the CX dosage. One can see that the increase in the CX dosage results in an increase in the phenol adsorption percentage. Phenol removal increases from 6 to 21.5 % when the adsorbent dosage increases from 0.025 to 0.2 g. This growth happened because the number of adsorption sites increased with the increase in the adsorbent dosage. With an increase in CX dosage from 0.175 to 0.2 g, the phenol adsorption percent slightly increased from 20.2 to 21.5 %. On the other hand, the total adsorbed amount of phenol (q_e) decreases from 60 to 27 mg g⁻¹ as the adsorbent dose increases from 0.025 to 0.2 g. The decrease in adsorption capacity with the increase in the adsorbent dosage is mainly attributed to the unsaturation of the adsorption sites through the adsorption process. Thus, the adsorbent dose was maintained at 0.075 g in all subsequent experiments, which was considered the best relation between the total adsorbed amount of phenol and percentage of removal.

3.3 Kinetic study

Figure 7 shows the phenol adsorption onto CX as a time function. The phenol concentrations used in the experiments were: 100, 300 and 500 mg dm⁻³. These curves show that the time required to reach the thermodynamic equilibrium depends on the initial phenol concentration, i.e. 15 min for a concentration of 100 mg L, 45 min for 300 mg L and 60 min for concentration equal to 500 mg L⁻¹.

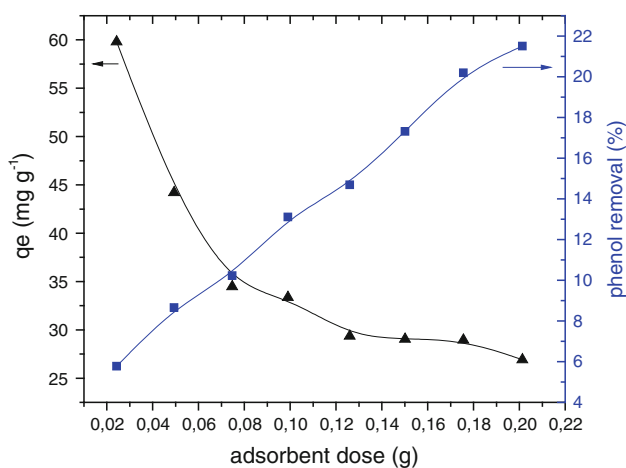


Fig. 6 Effect of adsorbent dose on the adsorption of phenol onto CX

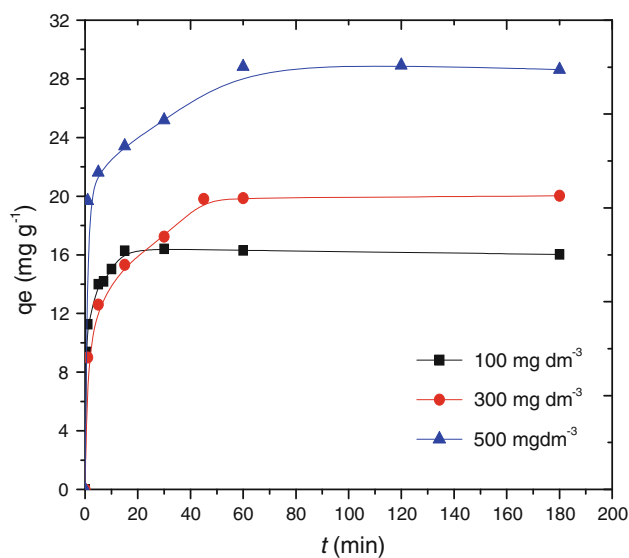


Fig. 7 Adsorption capacity variation with contact time in various initial phenol concentrations

The kinetic study was performed by fitting the experimental data to the pseudo-first-order, pseudo-second-order and diffusion intraparticle models [32].

The pseudo first-order model can be described by Eq. (1) [8]:

$$\log(q_e - q_t) = \log q_e - \frac{k_1 t}{2.303} \quad (1)$$

where, q_t and q_e are the mass of the adsorbed phenol at time t and at equilibrium, respectively, and k_1 is the rate constant of pseudo first-order adsorption process. The constants q_e and k_1 can be graphically determined by the plot $\log(q_e - q_t)$ versus t , where the slope is related to k_1 and the intercept is $\log(q_e)$.

The pseudo second-order model can mathematically be described by Eq. (2) [8]:

$$\frac{t}{q_t} = \frac{1}{k_2 q_e^2} + \frac{t}{q_e} \quad (2)$$

where, k_2 is the pseudo second-order rate constant and q_t and q_e were described previously. The constants of Eq. 2 can be graphically determined by the plot t versus (t/q_t) : the slope is related to the value of q_e , and the intercept is related to k_2 .

The intra particle diffusion model can be expressed by Eq. (3) [6]:

$$q_t = k_{in} t^{0.5} + c_b \quad (3)$$

where q_t is the mass of adsorbed phenol at time t , k_{in} is a kinetic constant, which is directly related with the intraparticle diffusion parameter and c_b is the thickness of the boundary layer. The values of the parameters k_{in} and c_b

can be determined by a plot of q_t versus $t^{0.5}$, where k_{in} is the slope and c_b is the intercept.

In Figs. 8 and 9 the experimental data were described by the linear form of the pseudo-first order and the pseudo-second order kinetic models, respectively. The constants obtained using the three models are listed in Table 1. The pseudo-first-order model gives poor fitting, with low R^2 values, and the q_e values estimated by this model substantially differ from those measured experimentally; suggesting that the adsorption is not a pseudo-first order reaction. However, Fig. 9 shows a good agreement of experimental data with the pseudo-second order model for different initial phenol concentrations. In addition, the calculated q_e values also agree well with experimental data. This indicates that the adsorption system studied belongs to the second order kinetic model. The equilibrium sorption capacities increased with the increase in phenol concentration. Nevertheless, the value of K_2 was found to decrease from 0.088 to 0.015 $\text{g mg}^{-1} \text{min}^{-1}$, for the increase in the initial concentration from 100 to 500 mg g^{-1} .

By the plots of q_t versus $t^{0.5}$, multilinearities were observed in Fig. 10, indicating that three steps took place [33]. The first portion (stage 1) can be attributed to the external surface adsorption, where adsorbate molecules diffuse through the solution to the external surface of adsorbent, to the boundary layer diffusion of solute molecules, where the adsorption rate is high. The second portion (stage 2) described by the gradual adsorption stage, where intraparticle diffusion was the limiting rate. The third portion (stage 3) was attributed to the final equilibrium stage for which the intraparticle diffusion started to slow down due to the low phenol concentration left in the solution. Therefore, the slope of the second linear portion may be defined as a rate parameter (k_{in}) and a characteristic of the adsorption rate in this region, where intraparticle

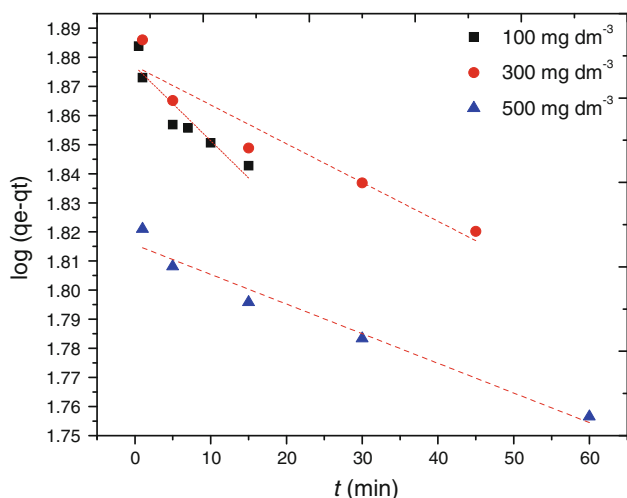


Fig. 8 Pseudo-first order kinetics for adsorption of phenol onto CX

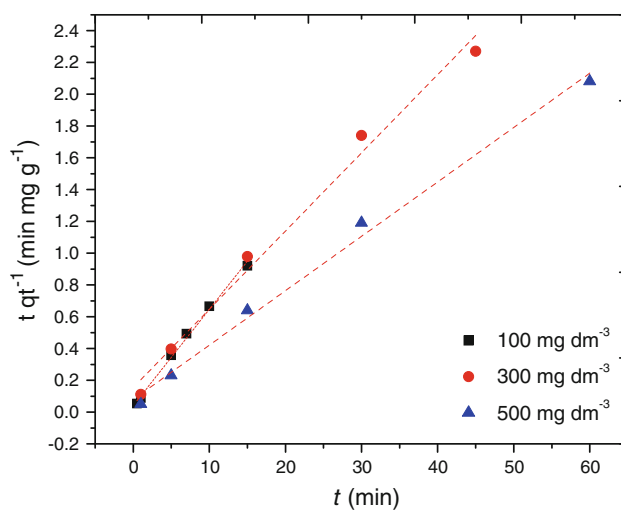


Fig. 9 Pseudo-second order kinetics for adsorption of phenol onto CX

diffusion has been reported to be the rate-limiting factor. As shown in Fig. 10, the external surface adsorption is absent for the highest concentration. For this concentration, stage 1 is completed before 1 min. If the intraparticle diffusion was the only rate-controlling step, the fitted line must pass through the origin of the plot. It can be seen in Fig. 10 that the plots don't pass through the origin, which means that the intraparticle diffusion is involved in the adsorption process but it is not the only rate-controlling step. That is, some other mechanisms such as the boundary layer diffusion may also control the rate of adsorption [33].

3.4 pH study

The pH value of phenol solutions plays an important role in the whole adsorption process and particularly in adsorption capacities. In this study, the effect of pH can be explained by considering the surface charge on the adsorbent and the phenol speciation.

The phenol removal quantity (q_e) in the pH range of 3–10 was displayed in Fig. 11. This Figure shows that q_e is constant and is in its maximum value at range of 3–8. However, after that the phenol removal decreased with the increase of pH. The point of zero charge (pH_{pzc}) of CX was here determined and is equal to 8.3. Therefore, the surface of CX at pH values lower than 8.3 is positively charged and at pH values higher than 8.3 are negatively charged. Phenol is a weak acid with $\text{p}K_a \sim 9.89$ [32] and is dissociated at $\text{pH} > \text{p}K_a$. Therefore, the phenol removal quantity (q_e) decreases at high pH values due to the electrostatic repulsions between the negative charge of CX surface and the phenolate anions in the solution [32]. While at pH values lower than 8.3, the percentage removal was higher because

Table 1 Kinetic parameters for phenol adsorption onto CX

Co (mg L ⁻¹)	Experimental data <i>q_e</i> (mg g ⁻¹)	First-order model			Second-order-model			Intraparticle diffusion	
		<i>K</i> ₁ (min ⁻¹)	<i>q_e</i> (mg g ⁻¹)	<i>R</i> ²	<i>K</i> ₂ (g mg ⁻¹ min ⁻¹)	<i>q_e</i> (mg g ⁻¹)	<i>R</i> ²	<i>k_d</i>	<i>R</i> ²
100	16.40	0.007	75.71	0.83	0.088	16.52	0.99	1.70	0.98
300	20.03	0.003	75.32	0.89	0.016	20.31	0.99	1.55	0.99
500	28.92	0.002	65.70	0.90	0.015	29.21	0.99	1.21	0.99

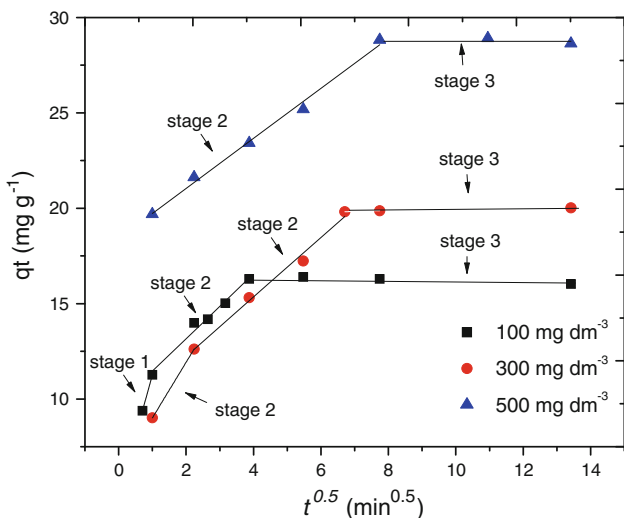


Fig. 10 Intraparticle diffusion kinetics for adsorption of phenol onto CX

phenol was mainly undissociated and the π–π dispersion interaction predominated.

3.5 Equilibrium adsorption

The equilibrium adsorption isotherm is essential for describing the interactive behavior between adsorbate and

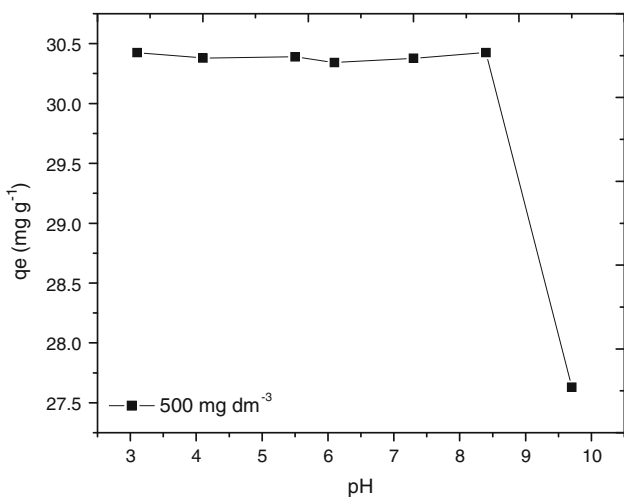


Fig. 11 Effect of solution pH on the adsorption of phenol onto CX

adsorbent. Langmuir and Freundlich isotherms are the most common ones. The Langmuir theory is valid for monolayer adsorption onto a surface containing a finite number of identical sites. Langmuir isotherm equation is expressed as [6]:

$$q_e = \frac{Q_m b C_e}{1 + q_e C_e} \tag{4}$$

where *q_e* is the amount adsorbed at equilibrium, *C_e* is the equilibrium concentration, *Q_m* (mg g⁻¹) is the maximum adsorption capacity and *b* is the binding constant which is related to the heat of adsorption. The Freundlich isotherm model is valid for heterogeneous surfaces. The Freundlich model is generally represented as follows [6]:

$$Q_e = K_F C_e^{1/n} \tag{5}$$

where, *C_e* is the equilibrium concentration, *K_F* and *1/n* are the Freundlich constants.

Figure 12 displays the adsorption isotherms of phenol onto CX. Adsorption of aromatic compound onto CX has been described by the Langmuir and Freundlich models [34].

The nonlinear least-squares regression was employed for data analyses and the results are presented in Table 2. It shows that Langmuir model fitted with *R*² close to 0.99. Therefore, Langmuir model described the data better than

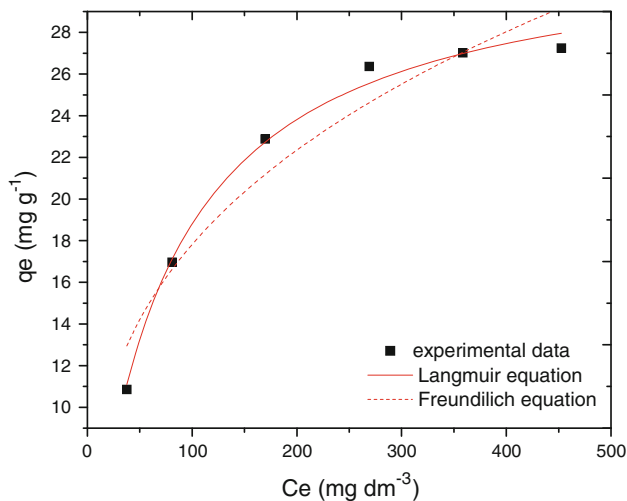
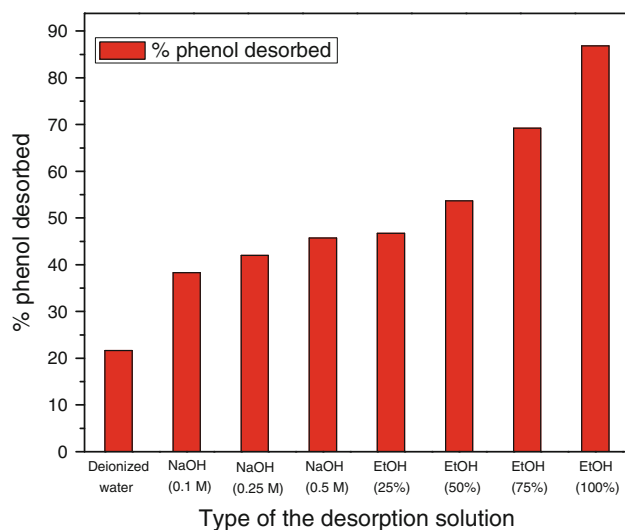


Fig. 12 Equilibrium adsorption isotherms of phenol onto CX

Table 2 Adsorption isotherms of phenol onto CX

Temperature (K)	Langmuir isotherm			Freundlich isotherm		
	b ($\text{dm}^3 \text{mg}^{-1}$)	Q_m (mg g^{-1})	R^2	K_L	$1/n$	R^2
298	0.014	32	0.99	4.0	0.327	0.92

**Fig. 13** Fraction of desorbed phenol from CX by different desorbing solutions

the Freundlich isotherm model. The monolayer adsorption capacity is 32 mg g^{-1} at 298 K.

3.6 Desorption

It is very important to regenerate the spent adsorbent for keeping the adsorption process cost down [8]. Desorption of phenol from loaded xerogel was carried out using different desorbing agents such as; deionized water, NaOH (0.1 M), NaOH (0.25 M), NaOH (0.5 M), EtOH (25 %), EtOH (50 %), EtOH (75 %), EtOH (100 %), in order to determine the most appropriate eluant or desorbing solution. The effect of type and concentration of desorbing agent in desorption process of phenol molecules onto xerogel is shown in Fig. 13. Among the desorbing solutions used in this study, the most efficient desorbent was EtOH (100 %) which released about 87 % of phenol bound with the CX. On the other hand, deionized water was identified as the worst eluent because of the desorption efficiency is 22 %. Experiments conducted with different concentrations of EtOH (25, 50, 75 and 100 %) showed that the percent desorption of phenol increase from 47 to 87 % with increase in concentration of the desorbing agent.

Table 3 Summary of adsorption capacity values of phenol on different activated carbons reported in literature

Adsorbent	Q_m (mg g^{-1})	Desorption (%)	Reference
Carbon xerogel	32	82	This work
Avocado activated carbon	90	38	[35]
Commercial activated carbon	32	–	[15]
Natural zeolites	35	–	[37]
Powdered activated carbon	13	–	[36]
Coconut shells activated carbon	34	–	[2]

Figure 13 also shows that the increase of NaOH concentration from 0.1 to 0.5 M has a slight influence on desorption capacity and efficiency.

Table 3 shows the maximum capacity values reported in literature for the adsorption and desorption of phenol on different materials; such adsorption data were also in this derived from the Langmuir equation. The maximum uptake of phenol reported in this paper (32 mg g^{-1}) is smaller than 90 mg g^{-1} observed for avocado kernels activated carbon (AAC) [35], higher than that reported for oil-palm empty fruit bunches activated carbon (13 mg g^{-1}) [36], and similar than those reported for phenol removal onto commercial activated carbon (32 mg g^{-1}) [15], coconut shells activated carbon (34 mg g^{-1}) [2] and natural zeolites (35 mg g^{-1}) [37], respectively. Although the phenol retention capacity displayed by carbon xerogel is lower than that achieved on avocado kernels activated carbon (AAC), the desorption value obtained in this paper is much higher than that one achieved by AAC [35]. Thus, the adsorption value attained by this product is high enough to consider its use in the purification of phenol in the industrial wastewaters and the desorption value attained is high enough for keeping the adsorption process cost down.

4 Conclusion

The Raman result indicates a carbon structure with a high content of lattice edges and plane defects. The BET surface area was found to be $128 \text{ m}^2 \text{ g}^{-1}$. The kinetic studies indicated that the adsorption of phenol molecules onto CX followed the pseudo-second order model and the intra particle diffusion process was the rate-controlling step. The optimum pH range ranges between 3 and 8. The optimum adsorbent dose obtained for phenol adsorption onto CX was 0.075 g. The equilibrium experimental data fitted very well with the Langmuir isotherm. For desorption of phenol 100 % EtOH solution was considered as the best desorbing agent.

Acknowledgments The authors gratefully acknowledge CAPES for financial support.

References

- Alkaram UF, Mukhlis AA, Al-Dujaili AH (2009) The removal of phenol from aqueous solutions by adsorption using surfactant-modified bentonite and kaolinite. *J Hazard Mater* 169:324–332
- Singh KP, Malik A, Sinha S, Ojha P (2008) Liquid-phase adsorption of phenols using activated carbons derived from agricultural waste material. *J Hazard Mater* 150:626–641
- Tor A, Cengeloglu Y, Ersoz M (2009) Increasing the phenol adsorption capacity of neutralized red mud by application of acid activation procedure. *Desalination* 242:19–28
- Tor A, Cengeloglu Y, Aydin ME, Ersoz M (2006) Removal of phenol from aqueous phase by using neutralized red mud. *J Colloid and Interface Sci* 300:498–503
- Hamdaoui O, Naffrechoux E (2007) Modeling of adsorption isotherms of phenol and chlorophenols onto granular activated carbon Part I. Two-parameter models and equations allowing determination of thermodynamic parameters. *J Hazard Mater* 147:381–394
- Liu QS, Zheng T, Wang P, Jiang JP, Li N (2010) Adsorption isotherm, kinetic and mechanism studies of some substituted phenols on activated carbon fibers. *Chem Eng J* 157:348–356
- Kumar A, Kumar S, Kumar S, Gupta DV (2007) Adsorption of phenol and 4-nitrophenol on granular activated carbon in basal salt medium: equilibrium and kinetics. *J Hazard Mater* 147:155–166
- Senturk HB, Ozdes D, Gundogdu A, Duran C, Soylak M (2009) Removal of phenol from aqueous solutions by adsorption onto organomodified Tirebolu bentonite: equilibrium, kinetic and thermodynamic study. *J Hazard Mater* 172:353–362
- Lin K, Pan J, Chen Y, Cheng R, Xu X (2009) Study the adsorption of phenol from aqueous solution on hydroxyapatite nanopowders. *J Hazard Mater* 161:231–240
- Kuleyin A (2007) Removal of phenol and 4-chlorophenol by surfactant-modified natural zeolite. *J Hazard Mater* 144:307–315
- Polat H, Molva M, Polat M (2006) Capacity and mechanism of phenol adsorption on lignite. *Int J Miner Process* 79:264–273
- Lua AC, Jia Q (2009) Adsorption of phenol by oil-palm-shell activated carbons in a fixed bed. *Chem Eng J* 150:455–461
- Dursun G, Çiçek H, Dursun AY (2005) Adsorption of phenol from aqueous solution by using carbonised beet pulp. *J Hazard Mater B* 125:175–182
- El-Naas MH, Al-Zuhair S, Alhaja MA (2010) Removal of phenol from petroleum refinery wastewater through adsorption on date-pit activated carbon. *Chem Eng J* 162:997–1005
- Stavropoulos GG, Samaras P, Sakellariopoulos GP (2008) Effect of activated carbons modification on porosity, surface structure and phenol adsorption. *J Hazard Mater* 151:414–421
- Meena AK, Mishra GK, Rai PK, Rajagopal C, Nagar PN (2005) Removal of heavy metal ions from aqueous solutions using carbon aerogel as an adsorbent. *J Hazard Mater* 122:161–170
- Wu X, Wu D, Fu R (2007) Studies on the adsorption of reactive brilliant red X-3B dye on organic and carbon aerogels. *J Hazard Mater* 147:1028–1036
- Kadirvelu K, Goel J, Rajagopal C (2008) Sorption of lead, mercury and cadmium ions in multi-component system using carbon aerogel as adsorbent. *J Hazard Mater* 153:502–507
- Lazarević S, Janković-Castvan I, Jovanović D, Milonjić S, Janačković D, Petrović R (2007) Adsorption of Pb^{2+} , Cd^{2+} and Sr^{2+} ions onto natural and acid-activated sepiolites. *Appl Clay Sci* 37:47–57
- Boehm HP (1966) *Advances in catalysis*, vol 16. Academic Press, New York
- Sharma CS, Kulkarni MM, Sharma A, Madou M (2009) Synthesis of carbon xerogel particles and fractal-like structures. *Chem Eng Sci* 64:1536–1543
- Dong-hui L, Jie Z, Jun-he Y, Zi-jun H, Tong-qi L, Guo C, Ruil Z, Li-cheng L (2008) Preparation and microstructure control of carbon aerogels produced using m-cresol mediated sol-gel polymerization of phenol and furfural. *New Carbon Mater* 23:165–170
- Stein A, Wang Z, Fierke MA (2009) Functionalization of porous carbon materials with designed pore architecture. *Adv Mater* 21:265–293
- Guilminot E, Fischer F, Chatenet M, Rigacci A, Berthon-Fabry S, Achard P, Chainet E (2007) Use of cellulose-based carbon aerogels as catalyst support for PEM fuel cell electrodes: electrochemical characterization. *J Power Sources* 166:104–111
- Lorjai P, Chaisuwan T, Wongkasemjit S (2009) Porous structure of polybenzoxazine-based organic aerogel prepared by sol-gel process and their carbon aerogels. *J Sol-Gel Sci Technol* 52:56–64
- Du J, Song C, Zhao J, Zhu Z (2008) Effect of chemical treatment to hollow carbon nanoparticles (HCNP) on catalytic behaviors of the platinum catalysts. *Appl Surf Sci* 255:2989–2993
- Sharma CS, Patil S, Saurabh S, Sharma A, Venkataraghavan R (2009) Resorcinol-formaldehyde based carbon nanospheres by electrospinning. *Bull Mater Sci* 32:39–246
- Job N, Pirard R, Marien J, Pirard J-P (2004) Porous carbon xerogels with texture tailored by pH control during sol-gel process. *Carbon* 42:619–628
- Sing KSW, Everett DH, Haul RAW, Moscou L, Pierotti RA, Rouquérol J, Siemieniewska T (1985) Reporting physisorption data for gas/solid systems with special reference to the determination of surface area and porosity. *Pure Appl Chem* 57:603
- Lee Y-F, Chang K-H, Chu C-Y, Chena H-L, Hu C-C (2011) Microstructure tuning of mesoporous silica prepared by evaporation-induced self-assembly processes: interactions among solvent evaporation, micelle formation/packing and sol condensation. *RSC Adv* 1:401–407
- Sevilla M, Fuertes AB, Mokaya R (2011) High density hydrogen storage in superactivated carbons from hydrothermally carbonized renewable organic materials. *Energy Environ Sci* 4:1400–1410
- Hameed BH, Rahman AA (2008) Removal of phenol from aqueous solutions by adsorption onto activated carbon prepared from biomass material. *J Hazard Mater* 160:576–581
- Cheung WH, Szeto YS, McKay G (2007) Intraparticle diffusion processes during acid dye adsorption onto chitosan. *Bioresour Technol* 98:2897–2904
- Dursun AY, Kalayci ÇS (2005) Equilibrium, kinetic and thermodynamic studies on the adsorption of phenol onto chitin. *J Hazard Mater B* 123:151–157
- Rodrigues LA, Silva MLCP, Alvarez-Mendes MO, Coutinho AR, Thim GP (2011) Phenol removal from aqueous solution by activated carbon produced from avocado kernel seeds. *Chem Eng J* 174:49–57
- Alam MZ, Muyibi SA, Mansor MF, Wahid R (2007) Activated carbons derived from oil palm empty-fruit bunches: application to environmental problems. *J Environ Sci* 19:103–108
- Yousef RI, El-Eswed B, Al-Muhtaseb AH (2011) Adsorption characteristics of natural zeolites as solid adsorbents for phenol removal from aqueous solutions: kinetics, mechanism, and thermodynamics studies. *Chem Eng J* 171:1143–1149